An Evaluation of Kernel-driven Bidirectional Models Using PARABOLA Measurements

by Z. Li • L. Moreau • J. Cihlar • D.W. Deering

RÉSUMÉ

Pour simuler la dépendance bidirectionnelle de la réflectance, l'utilisation de modèles bidirectionnels paramétriques (MBP) linéaires est de plus en plus courante. Cette étude est une évaluation de différents MBP effectuée en utilisant des données bidirectionnelles de réflectance de surface obtenues à l'aide d'un instrument appelé PARABOLA. Plusieurs essais ont été effectués en ajustant les MBP aux données de réflectance disponibles sur un domaine angulaire limité et non-limité, pour un angle zénithal solaire (AZS) fixe et variable, à la surface terrestre ainsi qu'au sommet de l'atmosphère. La performance de chacun des MBP est évaluée en comparant la corrélation entre la réflectance bidirectionnelle obtenue à partir des observations et celle simulée par les MBP de même qu'en comparant les albédos correspondants. Cette performance varie de façon considérable entre les MBP lorsque l'on restreint l'échantillonnage au plan principal. Lorsque les échantillons sont distribués sur le domaine angulaire complet, la plupart des MBP donnent un bon estimé de l'albédo; les erreurs relatives étant inférieures à 10%. Cependant, la dépendance bidirectionnelle simulée peut être très différente de la dépendance observée même si l'albédo simulé est bon. Des erreurs modérées se produisent lorsqu'un MBP ajusté pour un AZS spécifique est par la suite appliqué à d'autres AZS. La majorité des MBP performent mieux avec les données prises au sommet de l'atmosphère plutôt qu'au niveau du sol. La meilleure performance, pour le site à l'étude, a été obtenue en combinant l'équation paramétrique de Roujean et al. pour la diffusion de surface avec l'équation paramétrique de Ross pour la diffusion volumique. Cette combinaison permet d'obtenir des valeurs d'albédo ayant une erreur relative de seulement 2%.

SUMMARY

The kernel-driven bidirectional model (KDBM) is increasingly employed to account for the bidirectional dependence of reflectance. This study presents an evaluation of various KDBMs using surface bidirectional measurements acquired by PARABOLA. Numerous tests were conducted by fitting the KDBMs to reflectance data available in a limited and non-limited viewing domain for fixed and variable solar zenith (SZ) angles at the surface and top of the atmosphere (TOA). The performance was evaluated by comparing the fitness of observed bidirectional dependence and albedos from observations and KDBMs. Performance varies considerably among the KDBMs when samples are confined to such a limited domain as the principal plane where the NOAA/AVHRR data used in this study cover the northern regions. When the angular samples are distributed throughout the entire viewing domain, the majority of KDBMs offer good estimates of albedo with relative uncertainties of less than 10%, but fittings to the bidirectional dependence may differ drastically. Moderate errors ensue when a KDBM tuned to a specific SZ is applied to other SZ angles. Most KDBMs perform even better when applied to TOA measurements. The best performance, for the sites we investigated, is achieved by the combination of Roujean et al.'s surface scattering kernel and Ross' volume scattering kernel with a relative uncertainty in albedo estimate of a mere 2%.

• Z. Li and J. Cihlar are with the Canada Centre for Remote Sensing, 588 Booth Street, Ottawa, Ontario, K1A 0Y7

• L. Moreau is was with Intermap Tech., Ottawa, Ontario, and is now at 4735 Gobert Ave., Quebec, QC G1P 1G5

• D.W. Deering is with Biospheric Sciences Branch, Code 923, NASA Goddard Space Flight Center, Greenbelt, MD 20771 USA

INTRODUCTION

Optical remote sensing often deals with the angular dependence of reflectance as a function of viewing and illumination geometry, the so-called bidirectional reflectance distribution function (BRDF). BRDF is generally used to infer reflectance at a given viewing geometry and to compute an hemispheric albedo from a reflectance measurement made from a specific direction (Wu *et al.*, 1995). The former is needed for monitoring changes (Gutman, 1994), while the latter is an important geophysical parameter measuring the loss of solar energy in all directions. Due to technical difficulties in obtaining multi-angle measurements, BRDF has been the subject of extensive theoretical and empirical investigations for a long time (Strahler, 1994), but it still poses a significant problem (Li, 1996).

Various BRDFs have been put forward based on radiative transfer theories (Ross, 1981; Li and Strahler, 1986; Roujean *et al.*, 1992; Chen *et al.* 1996; etc.), observational data (Walthall *et al.*, 1985; Deering *et al.*, 1994; Cihlar *et al.*, 1994; etc.) and their combinations (Wu *et al.*, 1995; Wanner *et al.*, 1995; Li *et al.*, 1996). Kernel-driven BRDF (KDBM) is a typical hybrid model that is becoming increasingly popular. The kernels of the KDBMs generally originate from simplified treatments of the physical processes governing the radiative transfer and their coefficients are tuned from observations (Wanner *et al.*, 1995). In comparison to physical models, KDBMs contain few input parameters which can be inverted with minimal computation burden. Relative to empirical models, KDBMs are more flexible in terms of the number of observations required to determine model coefficients. Having these advantages, KDBMs are particularly suitable for operational use over large areas on a routine basis, such as for processing masses of Earth Observation System (EOS) data (Strahler *et al.*, 1995).

A successful use of a particular set of KDBMs (Roujean *et al.* 1992) was demonstrated with NOAA's Advanced Very High Resolution Radiometer (AVHRR) (Wu *et al.* 1995, Li *et al.* 1996). While the KDBM was found effective in accounting for the angular variation in the principal plane (the viewing domain of AVHRR in this region) (Li *et al.* 1996), the following important questions remain open:

(1) How well does the KDBM account for the dependence of reflectance on azimuth and solar zenith angles? This question is of direct consequence to the accuracy of an inferred albedo.
(2) How does this particular KDBM perform with respect to other KDBMs or, in general, which KDBM performs better? Answers to this question may depend on scene type.
(3) How do the KDBMs differ in performance when applied to reflectance measurements at the surface and top of the atmosphere (TOA) ?

This study attempts to address these questions by analyzing how KDBMs fit to some special ground measurements of bidirectional reflectance made during the Boreal Ecosystem-Atmosphere Study (BOREAS) (Sellers *et al.* 1995).

DATA

The data were acquired from the Portable Apparatus for Rapid Acquisition of Bidirectional Observations of the Land and Atmosphere (PARABOLA) designed by Deering and Leone (1986). PARABOLA is a motor-driven radiometer that allows reflectance measurements from different viewing directions during a very short period of time (~11 seconds). Under most circumstances, changes in surface and sky conditions of such short duration are negligible. PARABOLA has three spectral channels: red (650 – 670 nm), near infrared (810 – 840), and mid-infrared (1620 – 1690 nm). The first two fall within the spectral intervals of channels 1 and 2 of the NOAA AVHRR, respectively. Since the two AVHRR channels behave similarly in terms of bidirectional dependence (Wu *et al.*, 1995; Li *et al.*, 1996), only data in the red channel are analyzed here.

Bidirectional measurements were taken above three forest stands: old aspen (OA), old jack pine (OJP) and old black spruce (OBS) in the Southern Study Area (SSA) of the BOREAS. Since the sensor of PARABOLA was pointed to different locations when multi-angle measurements were made over the same stand, two measures were taken to lessen the impact of this limitation. First, the observation sites were selected in relatively homogeneous forest stands around the BOREAS flux towers. Second, multiple samples were taken from the same viewing direction by moving the instrument along a cable about 20 metres long and 14 metres above the top of canopies. Complete angular sampling at all angles was achieved at a 2-metre increment, leading to 11 data subsets for each observation period with an approximately constant sun angle. The replicated measurements of the same viewing geometry were then averaged. The footprint of the PARABOLA observation ranges from approximately 5.4 m^2 at nadir to approximately 46.6 m^2 at 60° degree off-nadir, which is larger than the size of most tree crowns. With these measures, uncertainties resulting from drifting observation spots are considerably suppressed, but not necessarily eliminated completely. The residual variations may introduce certain noise to the data, as is apparent in the later analysis.

Both original and aggregated PARABOLA data sets were available from the BOREAS Information System situated at the NASA/Goddard Space Flight Centre. The original data have varyied viewing angles, whereas the aggregated data are averaged in each of the 72 fixed bins of equal intervals in relative azimuth (30°) and view zenith (15°) for a given solar zenith (SZ). The bins of missing or bad data were substituted by either the data in opposite bins with respect to the principalplane (mirror symmetric assumption) or by the data interpolated from adjacent bins. SZ interval was set to be 5° starting from approximately 75° to the solar noon. Aggregated data collected during the first and second BOREAS intensive field campaigns encompassing the period May-July 1994 (IFC; Sellers *et al.*, 1995) were analyzed..

ANALYSIS

The KDBMs express reflectance (R) as linear combinations of two types of kernel functions denoting volume scattering (K_v) and surface scattering (K_s):

$$R = a + b\,K_{V,S}(\theta_i, \theta_v, \phi) \quad (1)$$

$$R = a + b\,K_V(\theta_i, \theta_v, \phi) + c\,K_s(\theta_i, \theta_v, \phi) \quad (2)$$

where θ_i, θ_v, ϕ represent three basic angles, namely, solar zenith, viewing zenith and relative azimuth, respectively. K_v accounts for the scattering caused by a collection of randomly dispersed facets of canopies and bare soils, while K_s for the diffuse reflection from opaque reflectors on the ground and the shadowing effects of leaves. $K_{V,S}$ denotes either of the two types. Use of a linear combination allows for quick inversion but probably at the expense of fitting accuracy, since the kernel functions are not mathematically diagonal (Gutman, private communication). The formats of five popular kernels including two for volume scattering and three for surface scattering are given in appendix, according to Wanner *et al.* (1995). The two volume scattering kernels were approximated from the canopy radiative transfer model developed by Ross (1981) for large and small leaf area index that are thereby designated as Ross-Thick and Ross-Thin kernels (Wanner *et al.* 1995). One surface scattering kernel was derived by Roujean *et al.* (1992), and two were simplified from the geometric optical model of Li and Strahler (1986, 1992) by Wanner *et al.* (1995) for sparse and dense forests. The performance of a KDBM given by Equations. (1) and (2) is evaluated under three scenarios.

Kernels fitted under restricted sampling conditions

In this case, the coefficients (a, b, c) of a KDBM were fitted using PARABOLA measurements in the principal plane (RA = 0° or 180°) for a given SZ. The fitted KDBM was then applied to all measurements of any viewing geometry for the same SZ. As stated in the introduction, the purpose of this test is to evaluate how well we can derive an albedo with minimal information concerning the BRDF as obtained from the NOAA/AVHRR whose viewing domain is close to the principal plane over the boreal forest region (Li *et al.*, 1996). Due to the limitation in angular sampling, the bidirectional effect can only be accounted for by assuming that the azimuthal dependence of a KDBM is correct. Since the bidirectional dependence is generally strongest in the principal plane, the constraint exerted by measurements in the principal plane may be most effective, relative to data available in other azimuthal planes

Figure 1 shows comparisons between observed and modeled reflectance for black spruce in three azimuthal planes, namely principal, perpendicular (RA = 90° or 270°) and diagonal (RA = 60° or 240°). Since the modelled values were computed with a KDBM tuned to observations in the principal plane, better agreement is found in this plane than in others. In the principal plane, the variation of reflectance with VZ is simulated well by almost all the two-kernel KDBMs, slightly worse by the single-kernel KDBMs with volume scattering kernels (Ross Thin and Thick), and worst by the surface scattering kernels. This finding is somewhat surprising, as we expected Li's kernels to perform better as they handle the shadowing effect between trees, whereas the Ross model deals with less-shadowing vegetation like grass. If the finding is true, it is presumably because the PARABOLA sensor placed above the forests is exposed primarily to tree crowns whose volume scattering outweighs the surface scattering effects due to branches and forest floor. The three forest stands exhibit similar angular trends, brighter in backward scattering direction than in forward scattering direction. Only one stand (OJP) displays the hot spot effect at the VZ equal to SZ (60°) which is captured by two KDBMs containing the Li-dense kernel. For other stands, the hot spot might be smoothed out as a result of averaging in the aggregated data. Relative to the two conifer forests, aspen has a more symmetrical distribution between forward and backward directions. This may be explained by the difference in tree structure. Aspen has a much more uniform tree crown than conifer forests do. The low leaf density and clustered shoots of conifer canopies produce many gaps that cast shadows in a forward scattering direction, leading to low reflectance. Significant disparities exist for comparisons in non-principal planes between observed and modeled reflectance (**Figure 1**). Although the shape of the angular variation does not differ very much between observations and 2-kernel KDBMs, the reflectance simulated by almost all KDBMs appears to be systematically larger than observations. This leads to positive bias errors in albedo estimates from the KDBMs, as seen clearly in **Figure 2** which shows the variation of relative error in albedo with SZ over three forest stands. Relative error (RE) is defined as

$$RE = (A_m - A_o)/A_o \quad (3)$$

where A_m and A_o denote modelled and observed albedo respectively. They were determined by integrating reflectance over the upper hemisphere from observations and models. The formula used to compute A_m for a KDBM is given in Li *et al.* (1996). Except for two KDBMs applied to OBS, positive bias errors dominate in all the comparisons. The relative difference in albedo ranges from 0 to up to 40% and has a relatively weak dependence on SZ. Different models behave more alike at lower SZ values. As expected, double-kernel KDBMs perform better (relative errors generally less than 20%) than single-kernel ones. The best performance was achieved over the aspen site with a relative error generally below 10%. Except for OBS, the KDBMs composed of the Roujean's surface scattering kernels have the lowest uncertainty (range 0 - 10%). The exception for OBS arises essentially from a peculiar bump of reflectance at small VZ angles in the backward scattering direction (c.f. **Figure 1**). There are no sound explanations but sampling errors, i.e. the measurements at different VZ angles may correspond to targets of significantly different reflectance.

Kernels fitted under optimal conditions

The second analysis was conducted by fitting the KDBMs to measurements in the entire viewing domain. This analysis aims to investigate the strengths and weaknesses inherent in a KDBM, as the limitation associated with data sampling is no longer a factor. Besides, the analysis has practical significance, since during the EOS era, observations from multiple viewing planes will be available (Strahler *et al.*, 1995). **Figure 3** presents the same results as **Figure 1** ,except all observations are

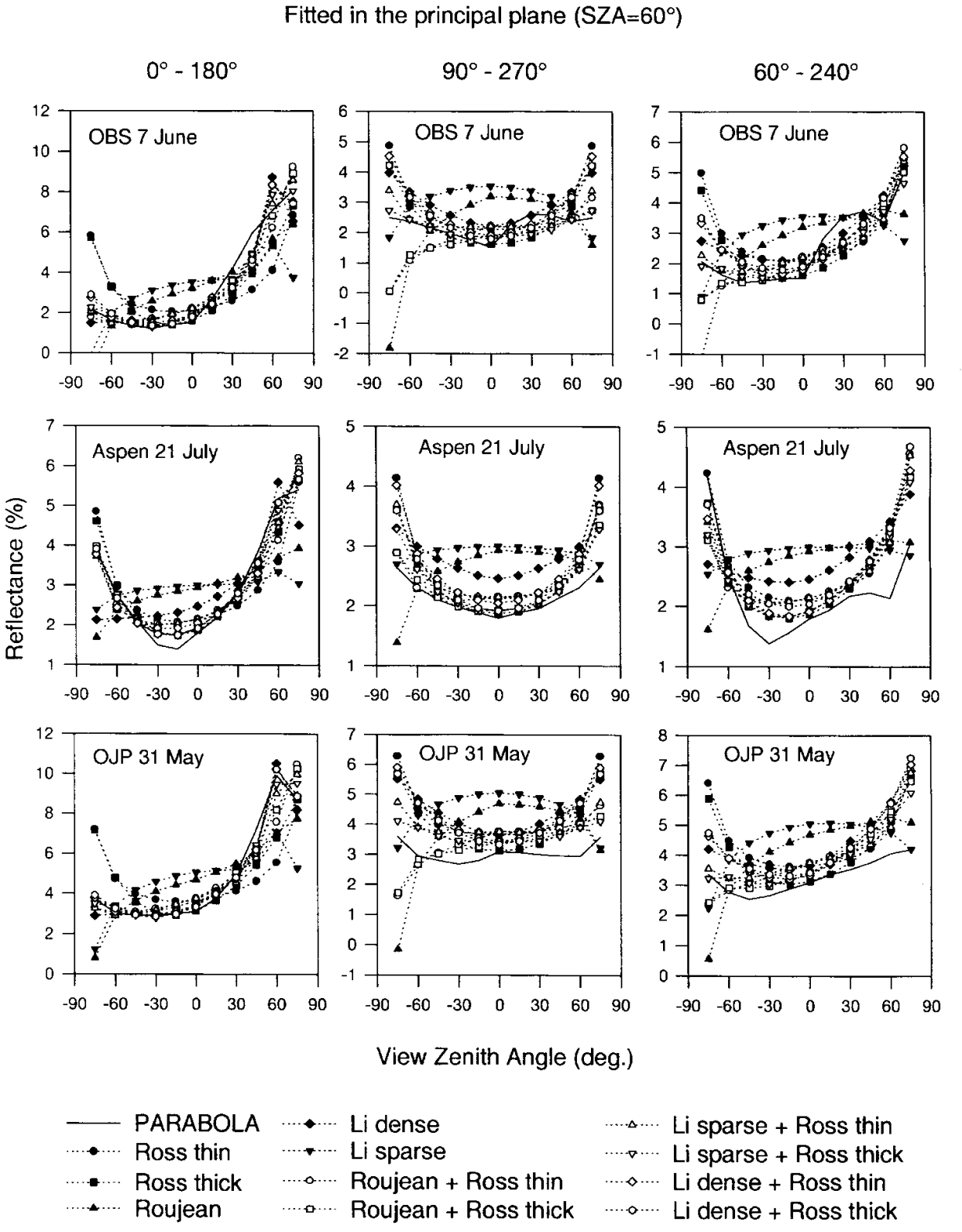

Figure. 1.
Variations of reflectance with viewing zenith in three observation planes of distinct relative azimuth angles (RAA): principal plane (RAA =0° or 180°), perpendicular plane (RAA =90° or 270°) and diagonal plane (RAA = 60° or 240°). The solid curve denotes observations obtained with PARABOLA and the dashed curves are the fits of the observations by various KDBMs.

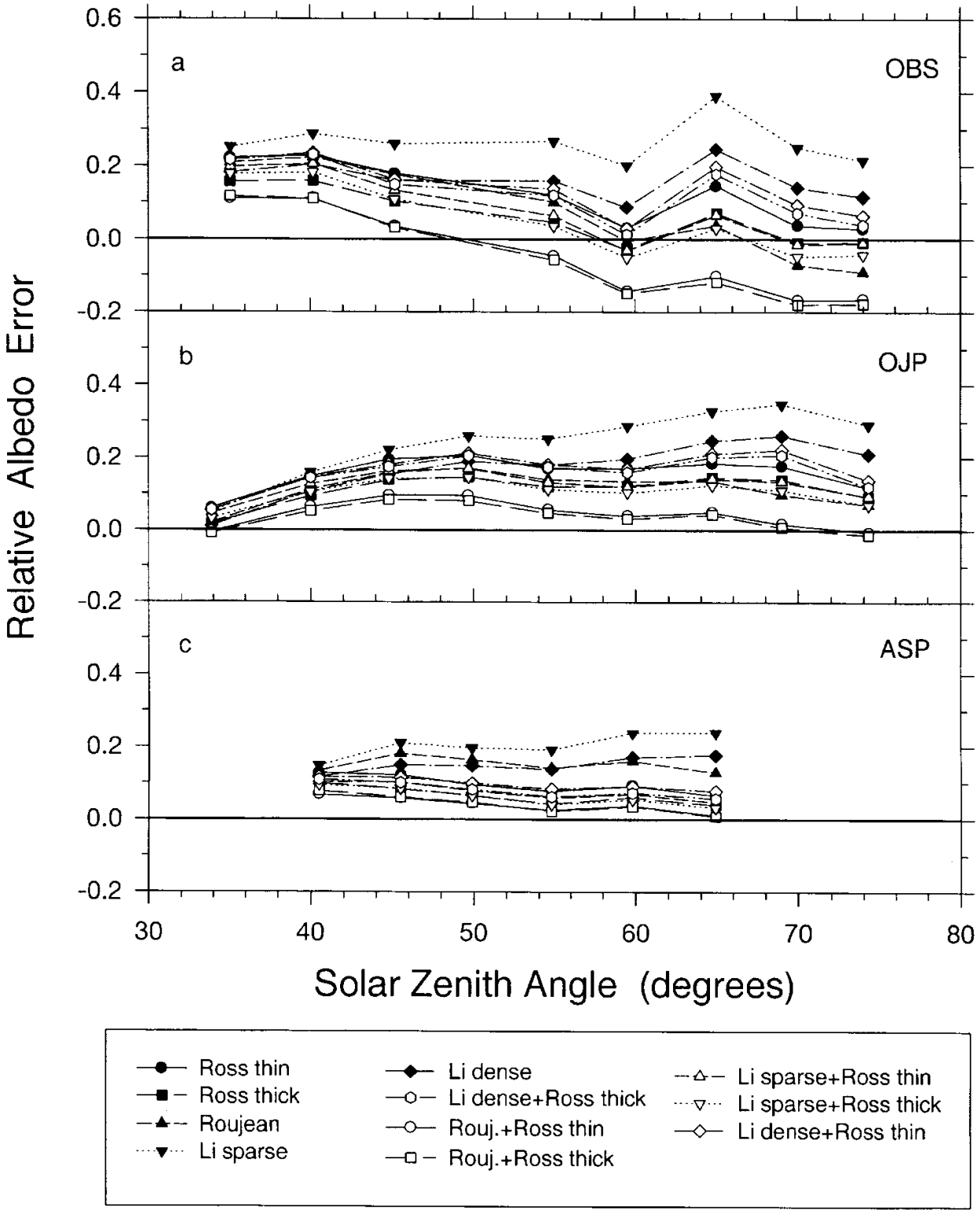

Figure 2.
Relative errors and their changes with solar zenith angle for the albedos derived from various KDBMs whose coefficients were fitted by the bidirectional measurements in the principal plane over old black spruce (OBS), old jack pine (OJP) and aspen (ASP) in the BOREAS northern study area.

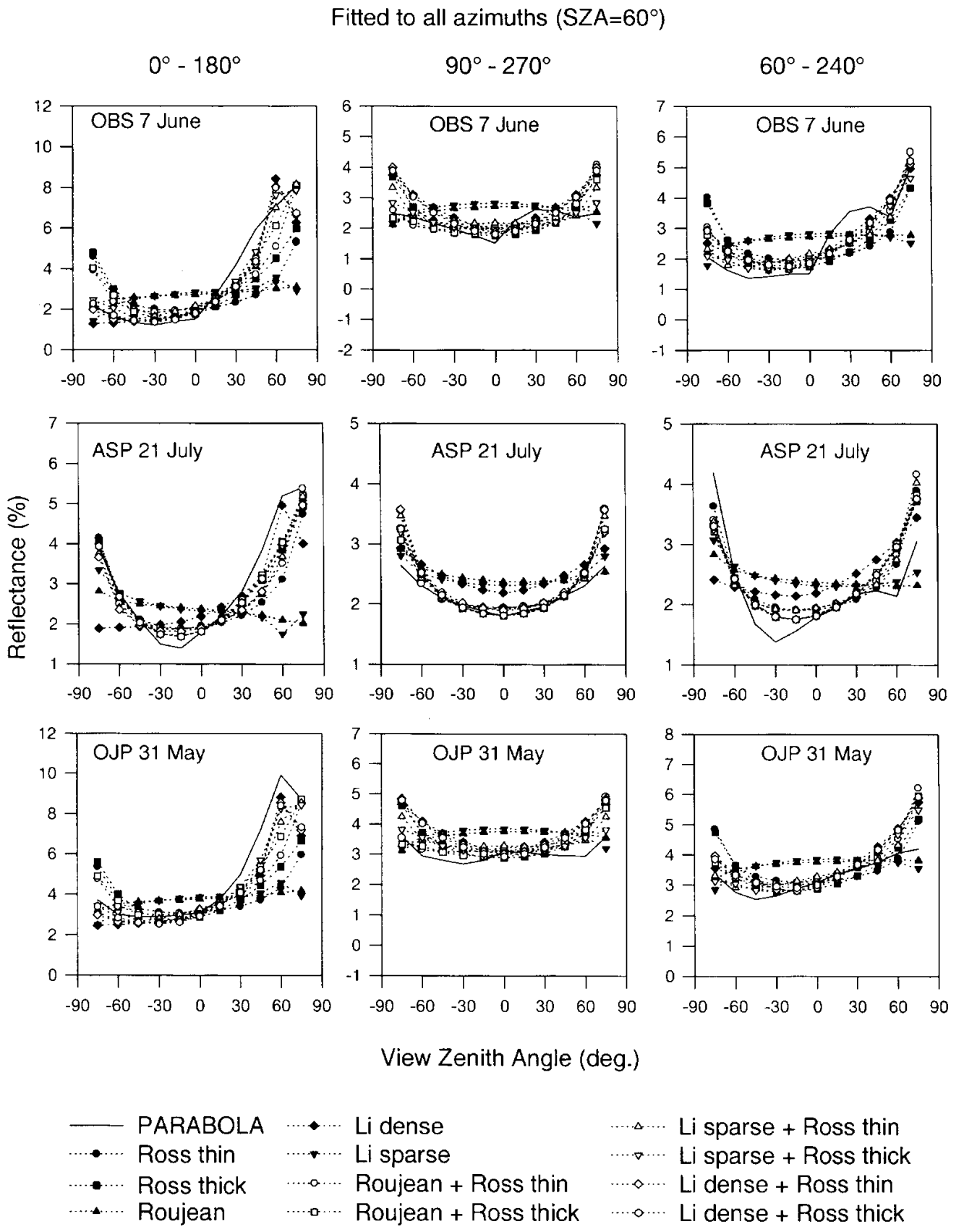

Figure 3.
Same as Figure 1 except that the KDBMs were fitted to the reflectance measurements made in the entire viewing domain.

used as input data. In comparison to **Figure 1**, some deterioration occurs in the principal plane but significant improvements in other planes. In particular, the KDBMs of double kernels substantially reduce the systematic errors in non-principal planes. Similar to the first analysis, good performance is attributed primarily to the use of volume scattering kernels.

Figure 4 shows the comparison of relative albedo errors computed from the KDBMs tuned to principal plane measurements and to all measurements. Only the results for the OBS comparison are shown here, since the comparisons for other sites are similar. The accuracy of albedo estimates increases substantially: most relative errors being less than 10%, compared to the original value of 30%. Intriguingly, the accuracy for single-kernel KDBMs is not significantly different from that for two-kernel KDBMs, although the fits are much worse for the former than for the latter (**Figure 3**). In fact, some single-kernel KDBMs such as the Roujean model lead to even more correct albedo estimates than combining with other kernels, e.g., the Roujean+Ross Thin or Roujean+Ross Thick. From the statistical point of view, this is not surprising, as the regression coefficients are determined by minimizing the variance (R^2) explained by the regression. It follows from **Figure 5** that the values of R^2 in the fitting of two-kernel KDBMs are always larger than single-kernel KDBMs. In particular, the R^2 for fitting the models of Roujean and Li Sparse is very low, but the errors in the resulting albedo are very small. This is simply because albedo is an integrated quantity and the errors in different parts of the viewing domain can offset each other. Thus, despite the poor performance in modeling the angular variation of reflectance by many single-kernel KDBMs (**Figure 3**), albedos resulting from these KDBMs may be good (**Figure 4**). It is worth noting that 10% relative uncertainty in albedo falls within the requirement of climate modelling (Li *et al.* 1997a)

This finding has an important implication. Derivation of albedo from a fitted KDBM is least sensitive to the selection of a KDBM when sufficient angular samples are available. In contrast, errors in the estimated albedos may differ dramatically from one KDBM to another for a limited number of samples, especially if they are restricted to a certain view domain, e.g. the principal plane. Unlike the derivation of albedo, normalization of reflectance to a common geometry depends critically on the quality of fitting over the entire viewing domain. It follows from **Figure 3** that substantial overestimation ensued from the use of single-kernel KDBMs that account for surface scattering only, unless their coefficients were fitted to a single plane and the ensuing KDBMs were applied to the same plane (Wu *et al.* 1995, Li *et al.* 1996).

The above analyses are for fixed SZ angles. For sun-synchronous satellites such as the NOAA series, measurements are made at about the same local time each day. Since albedo varies with SZ, knowledge of the dependence of albedo on SZ is required to infer albedos at other times in order to derive a daily mean albedo. Such knowledge is supposed to be "built-in"

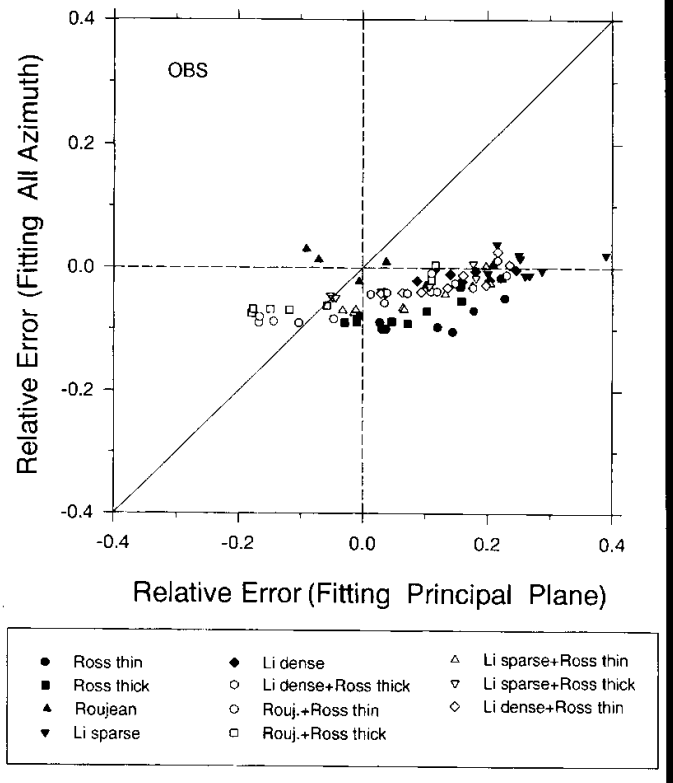

Figure 4.
Comparison of relative errors in the albedos estimated with KDBMs fitted by measurements made in the principal plane only and in all azimuthal planes over the OBS stand.

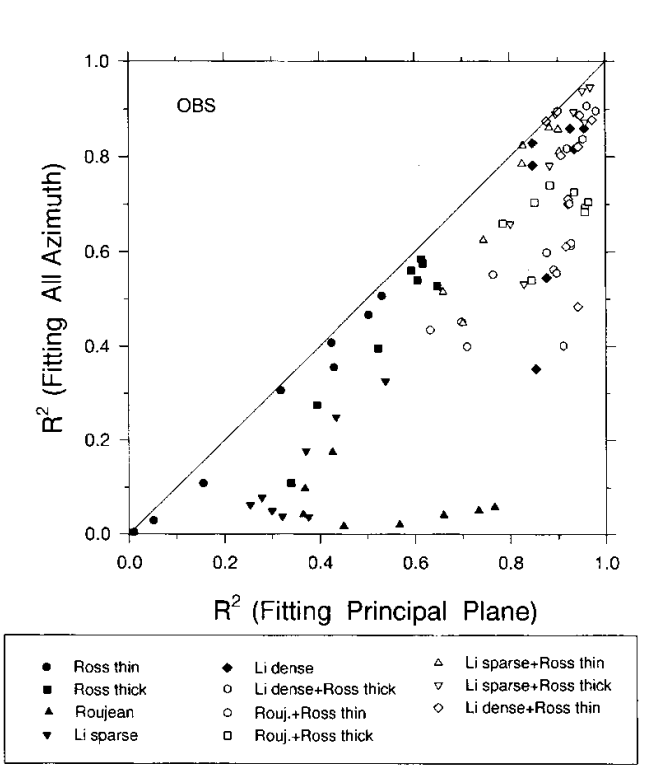

Figure 5.
Same as Figure 4 except for the variance explained by KDBMs.

the kernels which certainly deserves testing. To do so, we fitted the KDBMs with measurements at a fixed SZ and then applied them to estimate albedos at other SZ angles. The estimated albedos are compared with those derived from the KDBMs whose coefficients were tuned to actual SZ angles (c.f. **Figure 6**). Instead of plotting the two types of estimated albedos, **Figure 6** shows the comparison of the differences between estimated and observed albedos. Therefore, the distance to the "zero" lines measures absolute uncertainty and to the diagonal line (1:1) indicates the degradation of performance due to an imperfect treatment of the SZ dependence. The albedos estimated based on actual SZ angles are more accurate than those on a single SZ, but both tend to underestimte albedos as they have much more negative differences than positive ones. The degradation due to SZ dependence is further quantified by the standard deviations of the distance from data points to the diagonal line, as given in the parentheses beside the kernel names. The Roujean kernel appears to be most capable of accounting for the SZ dependence, followed by the Li sparse kernel. The two-kernel KDBMs are inferior to single-kernel ones in this regard.

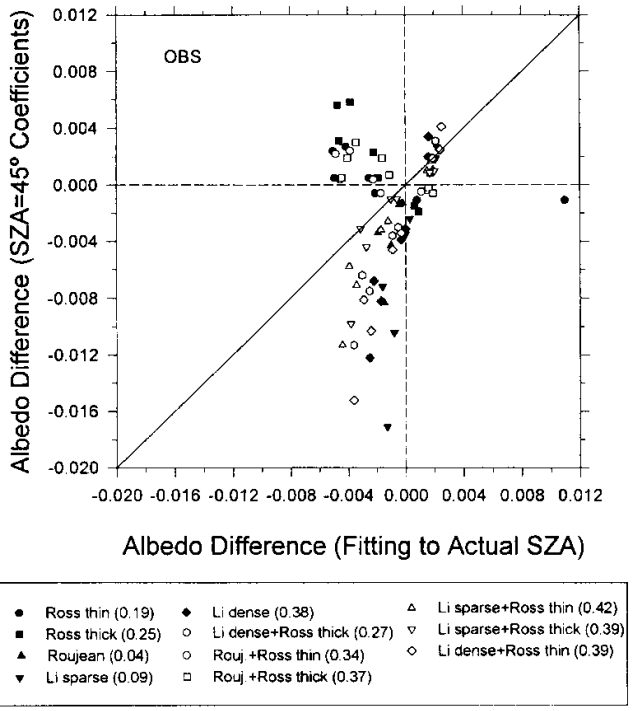

Figure 6.
The variance explained (a), standard deviation (b) and relative albedo estimation error (c) for the KDBMs fitted to the TOA reflectance data simulated with 6S over the OBS.

Kernels fitted to the TOA data

The third analysis was carried out with simulated reflectance at the top of the atmosphere (TOA). In principle, the kernels under study are valid at the surface, as they were obtained from simplification of the detailed models that were designed for treating specifically radiative processes within various surface media (Ross, 1981; Roujean *et al.*, 1992; Li and Strahler, 1986). While the Roujean+Ross Thick KDBM has been applied to TOA reflectance for correcting its dependence on viewing angle (Wu *et al.* 1995, Li *et al.* 1996), no efforts were made for other KDBMs. Moreover, it is worthwhile to compare the fitness of a KDBM applied to the same set of surface and TOA data.

Simulation of the TOA reflectance in AVHRR channel 1 (580 – 690 nm) was done with a modified version of the Second Simulation of the Satellite Signal in the Solar Spectrum (6S) (Vermote *et al.*, 1997). The 6S allows derivation of TOA reflectance from surface reflectance, or vice versa, by accounting for the effects of the intervening atmosphere due to Rayleigh scattering, water vapor absorption, aerosol scattering and absorption, etc. By incorporating the spectral filter functions of space-borne sensors, the reflectance in the bandpasses of radiometers such as the AVHRR can be computed directly. The main input data for the simulation include PARABOLA surface reflectance measurements, the corresponding viewing and illumination angles, and atmospheric properties for the middle latitude model summer atmosphere with a continental aerosol of optical thickness 0.1. The simulated data of TOA reflectance in the principal plane were then fitted by various KDBMs.

The results of fitting for OBS are presented in **Figure 7**. In comparison to the fitting at the surface as shown in **Figure 2**, TOA fits are even better. The relative uncertainties in albedo estimates are usually less than 10% for SZ<50 and larger at higher solar angles. Most accurate is the estimation by the Roujean+Ross Thick KDBM with a relative uncertainty of less than 2%, although the fit to the data is worse for this KDBM than for others (**Figure 7**).

To understand the effect of aerosol on the bidirectional dependence of TOA reflectance, simulations were carried out with varying aerosol optical thickness. **Figure 8a** presents the comparison of the dependence of reflectance on viewing zenith angle between surface PARABOLA measurements and TOA 6S simulation results at a SZ of 55°. The differences between the curves denote the contribution of the atmosphere and aerosol on BRDF. It is evident that both the atmosphere and aerosol enhance the angular dependence, especially towards high VZ angles in the forward scattering direction. The enhancement stems from the increase with VZ in the pathlength of solar photons due to Rayleigh scattering caused by the atmospheric molecules and Mie scattering by aerosol particles. Scattering in the atmosphere also attenuates the hot spot effect.

Shown in **Figure 8b** is the comparison between simulated and observed TOA reflectance. The AVHRR TOA reflectance measurements were acquired around the OBS flux tower on clear days during the period May to August 1994. The simulated TOA reflectance data were obtained by 6S with PARABOLA measurements as input values. While the angular variation in the simulated results is marked, the scatter is also prominent, especially at extreme angles. **Figure 8b** bears a close resemblance to **Figure 8a**, implying that the scattering of the reflectance measurements from AVHRR is caused primarily by the variation in aerosol loading. The summer of 1994 was an active fire season in and around the BOREAS study region

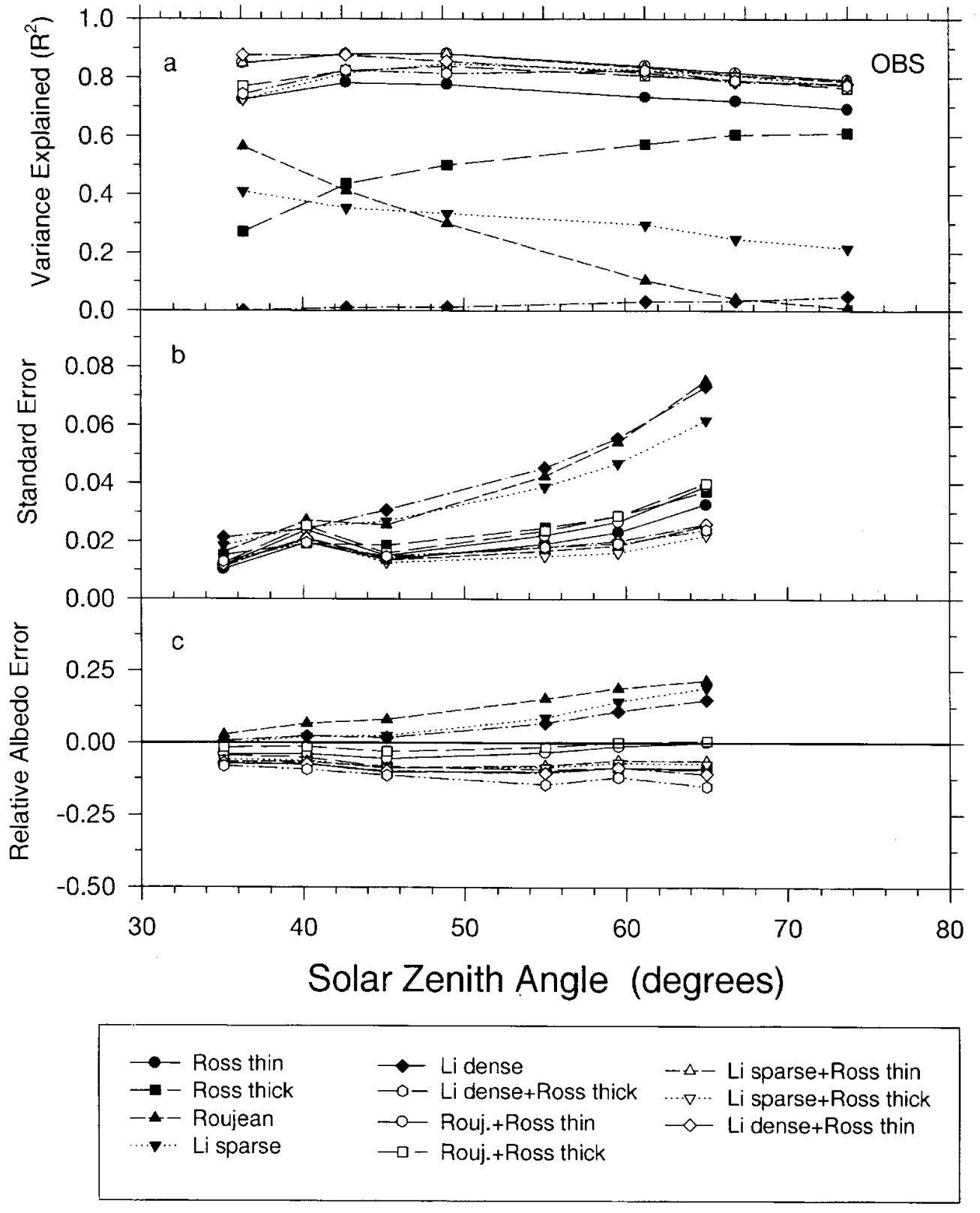

Figure 7.
Comparison of the differences between estimated and observed albedos. The estimated albedos were derived from two sets of KDBMs, one tuned to actual SZ angles and another to a fixed SZ at 45°. The numbers beside kernel names are the standard deviations of the data points to the diagonal line.

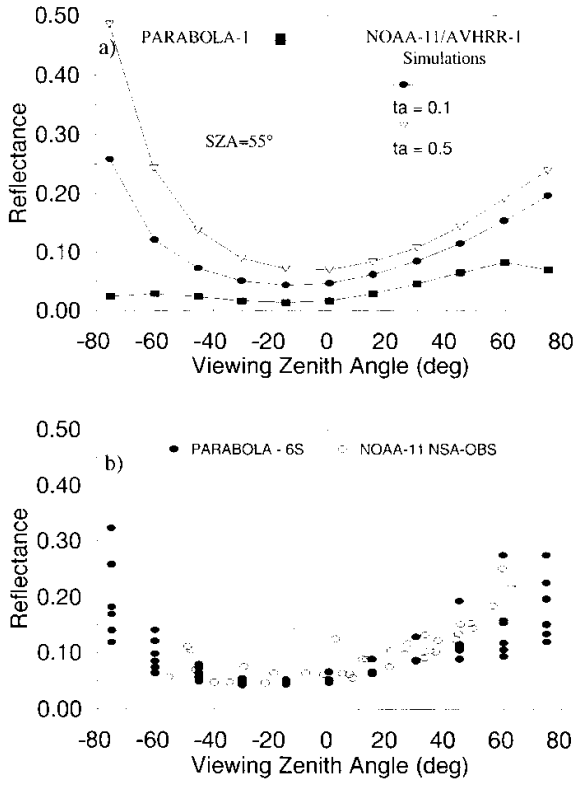

Figure 8.
Comparison of the dependence of reflectance on viewing zenith from observation and modeling. The three curves in the upper panel represent PARABOLA observations (rectangular), simulated AVHRR channel 1 reflectance with aerosol optical thickness 0.1 (circular) and 0.5 (triangle). The solid points in the lower panel are TOA reflectance simulated using PARABOLA surface measurements (for SZA between 40° and 65°) with 6S for varying aerosol optical thickness, while the open triangles are AVHRR actual measurements.

where about 2 million hectares of fires were detected from both space-borne and ground-based observations (Li *et al.*, 1997b). Due to the emission of smoke particles, aerosol optical thickness varies considerably from less than 0.1 (background aerosols) to over 5.0 (Markham *et al.* 1997). This leads to an unusually strong fluctuation in the TOA reflectance.

Summary

This study assesses the performance of an increasingly popular type of BRDF model, namely, the kernel-driven bidirectional model (KDBM). KDBM is a linear combination of one or two "kernels" derived from more detailed theoretical treatments of radiative transfer processes (Wanner *et al.* 1995). Eleven KDBMs composed of five kernels of two types describing volume and surface scattering processes were tested. The volume scattering kernels include Ross Thin and Ross Thick and surface scattering kernels encompass Roujean, Li Sparse and Li Dense (Wanner *et al.* 1995). Surface bidirectional reflectance measurements were employed that were acquired by the PARABOLA instrument above several boreal forest stands including old black spruce (OBS), old jack pine (OJP) and aspen (OA).

The KDBMs were evaluated under different scenarios. First, the coefficients of a KDBM were determined by fitting the KDBM to the PARABOLA measurements made in the principal plane wherein AVHRR sensors view the northern regions. The modelled and observed angular dependencies show significant discrepancy in non-principal planes, leading to systematic errors in the albedos derived from the KDBMs. The largest error occurs for a KDBM consisting of a single surface scattering kernel with relative positive bias errors up to 40%. Volume scattering kernels are more effective in reducing the uncertainties of albedo estimates. The relative uncertainties associated with a two-kernel KDBM containing a volume scattering kernel are less than 20%. The KDBM of Roujean + Ross Thin or Ross Thick has the least relative uncertainty (<10%). The second test tunes the coefficients of KDBMs to the PARABOLA measurements at all viewing angles. As envisioned, the fitness is improved in all viewing planes, except for the principal one. The ensuing albedo estimates are accurate to within 10%. Yet, the accuracy of albedo estimation is much less sensitive to the selection of KDBMs. When a KDBM tuned to measurements at a specific SZ is applied to measurements at other SZ angles, the resulting albedo estimates suffer large uncertainties, indicating inadequate treatment of the dependence on SZ. Relatively speaking, such a dependence is better handled by the Roujean kernel. The third test was applied to observed and simulated reflectance at the top of the atmosphere (TOA). Surface reflectance measurements from PARABOLA served as input for 6S to compute TOA reflectance. Surprisingly, the KDBMs fit TOA data better than surface data. The relative errors in TOA albedo estimates are generally less than 10% and the smallest is merely 2% for the Roujean + Ross Thick KDBM. Finally, the impact of the atmosphere and aerosol on the behavior of BRDF was investigated by changing aerosol loading in the 6S. The angular dependence and hot spot effect are dampened by these media.

Appendix: The BRDF Kernels Used in This Study

For convenience, given below are the formulae of various BRDF kernels under study. Details on each of the kernels can be found in Wanner et al. (1995).

i) Ross volume scattering kernels for thick and thin canopies

$$k_{Ross,\,thick} = \frac{\left(\frac{\pi}{2} - \xi\right)\cos\xi + \sin\xi}{\cos\theta_i + \cos\theta_v} - \frac{\pi}{4} \qquad \text{(A1)}$$

$$k_{Ross,\,thin} = \frac{\left(\frac{\pi}{2} - \xi\right)\cos\xi + \sin\xi}{\cos\theta_i \cos\theta_v} - \frac{\pi}{2} \qquad \text{(A2)}$$

$$\cos\xi = \cos\theta_i \cos\theta_v + \sin\theta_i \sin\theta_v \cos\phi \qquad \text{(A3)}$$

where ξ is the phase angle of scattering.

ii) Roujean surface scattering kernel (Roujean *et al.* 1992):

$$k_{Roujean} = \frac{1}{2\pi}[(\pi - \phi)\cos\phi + \sin\phi]\tan\theta_i \tan\theta_v - \frac{1}{\pi}(\tan\theta_i + \tan\theta_v + \sqrt{\tan^2\theta_i + \tan^2\theta_v\ \theta_v - 2\tan\theta_i \tan\theta_v \cos\phi}) \quad \text{(A4)}$$

iii) Li surface scattering kernels for sparse and dense canopies (Wanner *et al.*, 1995):

$$K_{Li,\,sparse} = O(\theta_i,\theta_v,\phi) - \sec\theta_i' - \sec\theta_v' + 0.5(1 + \cos\xi)\sec\theta_v') \quad \text{(A5)}$$

$$K_{Li,\,dense} = \frac{(1 + \cos\xi')\sec\theta'_v}{\sec\theta'_v + \sec\theta'_i - O(\theta_i,\theta'_v)} - 2 \quad \text{(A6)}$$

$$O = \frac{1}{\pi}(\mathrm{t} - \sin t \cos t)(\sec\theta'_i + \sec\theta'_v) \quad \text{(A7)}$$

$$\cos t = \frac{h}{b}\frac{\sqrt{D^2 + (\tan\theta'_i \tan\theta'_v \sin\phi)^2}}{\sec\theta'_i + \sec\theta'_v} \quad \text{(A8)}$$

$$D = \sqrt{\tan^2\theta'_i + \tan^2\theta'_v - 2\tan\theta'_i \tan\theta'_v \cos\phi} \quad \text{(A9)}$$

$$\cos\xi' = \cos\theta'_i \cos\theta'_v + \sin\theta'_i \sin\theta'_v \cos\phi \quad \text{(A10)}$$

$$\theta' = \tan^{-1}\left(\frac{b}{r}\tan\theta\right) \quad \text{(A11)}$$

where the two ratios, b/r and h/b, describe crown shape and relative height. For tall prolate canopies such as boreal forests, their values are set to be 2.5 (Wanner et al. 1995).

ACKNOWLEDGMENT

PARABOLA data were collected with the help of T. Eck. Constructive comments were made by J. Privette (NASA/GSFC). Editorial assistance was provided by C. Langham.

REFERENCES

Chen, J.M., and S.G. Leblanc, 1996. "A four-scale bidirectional reflectance model based on canopy architecture," *IEEE Trans. Geosci. & Rem. Sen.*, in press.

Cihlar, J., D. Manak, and N. Voisin, 1994. "AVHRR bidirectional reflectance effects and composite," *Remote Sens. Environ.*, vol. 48, pp. 77-88,
]

Deering, D.W., E.M. Middleton, and T.F. Eck, 1994. "Reflectance anisotropy for a spruce-hemlock forest canopy," *Rem. Sen. Environ.*, 47:242-260.

Gutman, G., 1994. "Normalization of multi-annual global AVHRR reflectance data over land surfaces to common sun-target-sensor geometry," *Adv. Space Res.*, 14:121-124.

Li, X. and A. H. Strahler, 1986. "Geometric-optical bidirectional reflectance modelling of a conifer forest canopy," *IEEE Trans. Geosci. Remote Sens.*, GE-24: 906-919.

Li, Z., J. Cihlar, X. Zhang, L. Moreau, L. Hung, 1996. "The bidirectional effect in AVHRR measurements over boreal regions,"*IEEE Tran. Geosci. & Rem. Sen.*, 34:1308-1322.

Li, Z., 1996. "On the angular correction of satellite-based radiation data: An evaluation of the performance of ERBE ADM in the Arctic," *J. Theor. Appl. Climat.* 54: 235-248.

Li, Z., L. Moreau, A. Arking, 1997a. "On solar energy disposition, A perspective from observation and modeling," *Bull. Amer. Meteor. Soc.*, 78:53-70

Li, Z., J. Cihlar, L. Moreau, F. Huang, B. Lee, 1997b. "Monitoring fires in the boreal ecosystem," *J. Geophy. Res.* In press.

Markham, B.J., J.S. Schafer, B.N. Holben, and R.N. Halthore, 1997. "Atmospheric aerosol and water vapor characteristics over north central Canada during BOREAS," *J. Geophy. Res.*, in press.

Ross, J.K. 1981. *The radiation regime and architecture of plant stands*, Dr. W. Junk Publishers, The Hague, 392 pp.

Roujean, J. L., M. Leroy, A. Leroy, and P. Y. Deschamps, 1992. "A Bidirectional Reflectance Model of the Earth's Surface for the Correction of Remote Sensing Data, *J. Geophy. Res.*, 97: 20455-20468.

Sellers, P., F. Hall, H. Margolis, B. Kelly, D. Baldocchi, G. den Hartog, J. Cihlar, M.G. Ryan, B. Goodison, P. Crill, K.J. Ranson, D. Lettenmaier, and D.E. Wickland, The boreal ecosystem-atmosphere study (BOREAS): An overview and early results from the 1994 field year, *Bull. Am. Meteorol. Soc.*,76, 1549-1577, 1995.

Strahler, A.H., 1994. "Vegetation canopy reflectance modeling - Recent developments and remote sensing perspectives," *Proc. Sixth. Inter. Symp. on Phys. Measures and Signature*, Val d'Isere, France, 17-21 January, pp. 593-600.

Strahler, A, and 9 Team Members, 1995. "MODIS BRDF/Albedo product: Algorithm theoretical basis document, Version 3.2," Boston Univeristy, pp 86.

Vermote, E.F., D. Tanre, J.J. Morcrette, J.L. Deuze, M. Herman, 1997. "Second simulation of the satellite signal in the solar epectrum: An overview," *IEEE Trans. Geosci. Rem. Sens.*, 35: 675-686.

Walthall, C.L., J.M. Norman, J.M. Welles, G. Campbell, and B.L.Blad, 1985. "Simple equation to approximate the bidirectional reflectance from vegetative canopies and bare soil surfaces," *Applied Optics*, 24: 383-387.

Wanner, W., X. Li, and A.H. Strahler, 1995. "On the derivation of kernels for kernel-driven models of bidirectional reflectance," *J. Geophy. Res.*, 100: 21,077-21,089.

Wu, A., Z. Li, and J. Cihlar, 1995. "Effects of land cover type and greenness on advanced very high resolution radiometer bidirectional reflectances: Analysis and removal," *J. Geophy. Res.*, 100: 9179-9192, 1995.